Long term irradiance clear sky and all-weather model validation

Ineichen, Pierre

SASEC2016
4TH SOUTHERN AFRICAN SOLAR ENERGY CONFERENCE
31Oct - 2 Nov 2016 | Stellenbosch, South Africa

LONG TERM IRRADIANCE CLEAR SKY AND ALL-WEATHER MODEL VALIDATION

Pierre Ineichen[1]

[1] University of Geneva, Institute for environmental sciences, Energy system group, 66 bd Carl-Vogt, 1211 Geneva 4, Switzerland;
Phone +41223790640; e-mail: pierre.ineichen@unige.ch

Abstract

The optimal utilization of solar energy requires a thorough characterization of the solar resource. The most accurate way is to measure that resource in situ. However accurate measurements are not a common commodity, especially over longer time spans. To circumvent the lack of ground-based measurements, models can be applied to estimate solar irradiance components. A fundamental component is the clear sky irradiance. In particular, clear sky irradiance is used as the normalization function in models that convert meteorological satellite images into irradiance.

This paper presents the results of a validation of models that evaluate solar irradiance based on satellite images spanning up to 8 years. The validation relies on high quality measurements from 24 sites in Europe and Africa. After a thorough assessment of the ground measurements, clear conditions are selected in the data banks to evaluate the performance of seven clear sky models. Finally, seven satellite all-weather models are validated against the ground data.

Keywords: satellite derived irradiance; clear sky model; hourly, daily and monthly data; interannual variability; validation

1. Introduction

The meteorological satellite images as data source to evaluate the ground irradiance components become the state of the art in the field of solar energy systems. The strongest argument is the high spatial coverage, and the fifteen minutes temporal granularity when using images from MSG. They also have the advantage to provide real time data used for example to assess the proper operation of a solar plant. On the other hand, long-term ground data are very scarce concerning the beam irradiance. The use of secondary inputs such as polar satellite data and ground information increases significantly the precision of the algorithms, mainly for the beam component. Following a paper from Zelenka concerning the nuggets effect, the interpolation distance to the nearest ground measurement site is limited to 10 to 30 km, depending on the irradiance parameter. This strengthens the satellite derived data argument. Clear sky models are part of the process and therefore have to be thoroughly validated.

The use of data derived from models or interpolated between nearby measurements sites are strongly related to the quality of the ground measurements used in the deriving process. This means that the preparatory steps are essential to ensure the quality of the data to be used as input to system simulations.

Our approach is to first apply a stringent quality control, including time stamp of the data, absolute and relative calibration coefficient of the sensors, long term stability, components coherence etc., on the ground and modelled data.

The usual statistical indicators such as mean bias, root mean square deviation, standard deviation of the bias, correlation coefficient, etc. are used to benchmark the product. We also applied a second order statistic to characterize the frequency distributions. The comparison is done on an hourly, daily, monthly and yearly basis, on both the global and the beam components. The interannual variability is also studied.

2. Ground data

Data from 24 ground stations are used for the validation, with up to 25 years of continuous measurements; for the validation itself, due to the satellite data availability, only data from 2004 to 2015 are used. The data acquired before the reference period are used to evaluate the interannual variability. The climate range mainly covers desert to oceanic, latitude up to 60°N, and altitudes from sea level to 1600 meters. The latitude, altitude and climate of the selected sites are given on Table 1.

The concerned parameters are the global irradiance on a horizontal plane G_h, the normal beam irradiance B_n and the horizontal diffuse irradiance D_h. For some sites, only the beam or the diffuse component is acquired; the third component is then calculated by difference following the closure equation, the equation connecting together the three irradiance components: $G_h = D_h + B_n \sin(h)$, where h is the solar elevation

angle. For one site, the South African site of Skukuza, only the global component is available. For comparison purpose, the beam component is evaluated with the help of the DirIndex model (Perez 1992).

Site	Lat.	Alt.	Climate
Almeria	37.092	491	dry, hot summer
Bratislava	48.166	195	semi-continental
Cabauw	51.97	70	temperate maritim
Camborne	50.22	88	oceanic
Carpentras	44.083	100	mediternean
Davos	46.813	1586	alpine
Geneva	46.199	420	semi-continental
Kassel	51.312	173	temperate humide
Mt Kenya	-0.062	3678	warm humid
Kishinev	47	205	continental humid
Lerwick	60.133	82	cold oceanic
Lindenberg	52.21	125	moderate maritim
Madrid	40.45	650	semi-arid
Nantes	47.254	30	oceanic
Payerne	46.815	490	semi-continental
Sede Boqer	30.905	457	dry steppe
Stellenbosch	-33.917	128	temperate, hot summer
Skukuza	-25.02	365	steppe, hot arid
Tamanrasset	22.78	1400	hot, desert
Toravere	58.254	70	cold humid
Valentia	51.938	14	oceanic
Vaulx-en-Velin	45.778	170	semi-continental
Wien	48.25	203	continental
Zilani	56.52	107	cold humid

Table 1. Ground measurements sites

3. Description of the models

3.1. Clear sky models

Seven of the best-performing and/or widely used models are selected for evaluation. The choice of models is based on their performance, their ease of use and their computation speed. These models require aerosol optical depth (*aod*) and water vapour column (*w*) as an input. Two of the models need Linke turbidity coefficient at air mass 2 as an input.

McClear: it is a fully physical model developed by Mines Paris Tech (Lefèvre 2013). The core of the model consists of look-up tables (LUT) calculated with the LibRadTran Radiative Transfer Model (RTM) (Mayer 2005) in a 10-dimensions space including aerosol optical depths at two wavelengths, partial aerosol optical depths for the determination of the aerosol type, the water vapour column and the ozone amount. The model uses the parameters derived from the MACC-II project.

Simplified Solis: based on the original Solis spectral model (Mueller 2004), it consist of a broadband fit on LibRadTran calculations in a 10-dimensions space including aerosol optical depths, water vapour column and ozone amount (Ineichen 2008a). The model includes rural, urban, maritime and tropospheric aerosol types. The model requires panchromatic aerosol optical depth and water vapour column as inputs.

CPCR2: a physical model, parametrized in two solar spectrum bands. In each band a radiation modelling technique is applied and a transmittance of each extinction layer is parametrized to derive transmission functions for the beam and the diffuse components of the clear sky irradiance. The main input parameters to the model are the two Angström coefficients (the exponent alpha, or the size parameter, and the turbidity coefficient beta) and the water vapour column *w* (Gueymard 1989).

REST2: a two-bands model that uses the general features of CPCR2 with updated transmittance functions calculated with the SMARTS spectral model (Gueymard 2001) and using the latest extra-atmospheric spectral distribution and solar constant value. The input parameters are the same than for CPCR2 (Gueymard 2004).

Bird: based on Radiative Transfer Model calculations with SOLTRAN (RTM scheme constructed from LOWTRAN) (Bird 1980). The model requires three input parameters: the water vapour column *w*, the broadband aerosol optical depth *aod* (at 700), and the total ozone column O_3 considered here as constant and equal to 340 Dobson units.

ESRA: developed in the frame of the European Solar Radiation Atlas (ESRA 2000). Contrary to other models, it derives separately the beam and the diffuse components that are added to obtain the global irradiance. The beam component is based on Kasten's Rayleigh optical depth parametrization and on the Linke turbidity (Kasten 1996). The clear sky diffuse irradiance is expressed as the product of a zenith diffuse transmission and a diffuse angular function.

Kasten: based on the pyrheliometric formula from Kasten (1980). The irradiances are calculated by taking into account the absorption and scattering at two altitude levels: 2.5km and 8km (Kasten 1984). The model uses the Linke turbidity to parametrize the aerosol load and water vapour of the atmosphere.

The last model, based on Linke turbidity coefficient is included in the study for comparison purpose.

3.2. All-weather satellite (or now casting) models

For the real time (or now casting) model comparison, seven different products are validated in the present study. The methodology and their input parameters are the following:

SolarGis: the irradiance components are the result of a five steps process: a multi-spectral analysis classifies the pixels, the lower boundary evaluation is done for each time slot, a spatial

variability is introduced for the upper boundary and the cloud index definition, Solis clear sky model is used as normalization, and a terrain disaggregation is finally applied.

Helioclim-3: it is based upon calibrated radiances from the satellite. The use of known models of the physical processes in atmospheric optics removes the need of empirically defined parameters and of pyranometric measurements to tune them. ESRA models (ESRA 2000, Rigollier 2000 and 2004) are used for modelling the clear-sky irradiation, the turbidity is based on climatic monthly Linke turbidity coefficients data banks. Liu and Jordan model is used to split the global irradiance into the diffuse and beam components (Liu 1960).

Solemi: for the global irradiance G_h, an algorithm based on the Heliosat method (Cano 1986, Hammer 2000 and 2003) is implemented. The beam component B_n is directly derived from the satellite images by the method of Schillings (2003). Instead of using a general turbidity, each important constituent is treated separately with the help of Bird clear sky model. The cloud parameterization scheme is a two-channel procedure, which uses the visible and the infrared channels of Meteosat.

IrSOLaV: the cloud index n is derived using the Dagestad method (Dagestad 2007), the ground albedo is computed from a forward and backward moving window of 14 days taking into account its evolution during the day, as function of the co-scattering angle. G_h is then evaluated from the cloud index with the Zarzalejo model (Zarzalejo 2009) and B_n from the global irradiance with Louche's correlation (Louche 1991). ESRA clear sky model is used in the scheme, using aerosol optical depth *aod* from Soda, MODIS or from Polo, 2009.

EnMetSol: it is based on the Heliosat method. Two different clear sky models are used in the scheme: the model of Dumortier (Fontoynont 1998, Dumortier 1998) with the Remund (2009) Meteonorm data base for the turbidity input, and the spectral Solis clear sky model (Mueller 2004) with monthly averages of *aod* (Kinne 2005) and water vapour content (Kalnay 1996) as input. For Dumortier clear sky, a diffuse fraction model (Lorenz 2007) is used to calculate the all sky diffuse horizontal irradiance (via G_h and B_n). A recently developed beam fraction model (Hammer 2009) is used to calculate the B_n for all sky conditions with the Solis model.

HelioMont: the scheme is based on the Heliosat method adapted for the Meteosat satellite by MeteoSwiss (Möser 1984, Stoeckli 2013). For bright surfaces, the infrared cloud index replaces the visible (classical) cloud index. This guarantees that the clear sky reflectance and brightness temperature values have consistency on the diurnal time scale. This also enables to account for short-term changes in surface reflectance, such as during green-up or during periods of snow fall. In HelioMont the maximum cloud reflectance fields are calculated with a radiative transfer model simulating the radiative properties of ice and water clouds with an optical thickness of 128 at each time step (Mayer 2005).

CAMS: new version of Helioclim model based on MACC-II aerosol load and McClear clear sky model (Oumbe 2014). The method is based on the approximation that the solar irradiance at ground level is obtained from the product of the irradiance under clear atmosphere and a modification factor due to cloud properties and ground albedo only.

3.3. Average and typical years

Depending on the application, average or typical years are used as input to simulations. These are generally obtained from 10-20 years of measurements, averaged, partially interpolated and/or satellite based. Some of them are corrected with data from meteorological and polar satellite data and/or ground informations. The data included in the comparison are derived from networks or software and are described below.

PVGIS: PhotoVoltaic Geographical Information System provides a map-based inventory of solar energy resource and assessment of the electricity generation from photovoltaic systems in Europe, Africa, and South-West Asia.

WRDC: the World Radiation Data Centre online archive contains international solar radiation data from over one thousand measurement sites throughout the world.

RetScreen: worldwide data bank to evaluate the energy production and savings, costs, emission reductions, financial viability and risk for various types of renewable-energy and energy-efficient technologies.

NASA SSE: satellite based energy resource web site of global meteorology and surface solar energy climatology from NASA with a spatial resolution of 1 by 1 degree.

Meteonorm: meteorological reference software, based on more than 20 years of measurements and satellite data.

ESRA: European Solar Radiation Atlas, based on the best ground measurements complemented with other meteorological data necessary for solar engineering. Digital maps for the European continents and monthly tables are produced.

For the seven now casting modelled data sets described in section *3.2*, the data are either aggregated into monthly values, or directly retrieved from the provider in monthly values.

4. Ground measurements quality control (QC)

The validity of the results obtained from the use of ground measured data is highly correlated with the quality of the data

bank used as reference. Controlling data quality is therefore the first step to perform in the process of validating models against ground data. This essential step should be devised properly and automated in order to rapidly detect significant instrumental problems like sensor failures or errors in calibration, orientation, levelling, tracking, consistency, etc. Even if some QC procedures have been implemented by the group in charge of the acquisition, it might not be sufficient to catch all errors, or the data points might not be flagged to indicate the source of the problem. A stringent quality control procedure must therefore be adopted in the present context, and its various elements are described in what follows.

An a posteriori automatic quality control cannot detect all acquisition problems that could have happened, however. The remaining elements to be assessed are threefold:

- the measurement's time stamp (needed to compute the solar geometry),
- the sensors' calibration coefficient used to convert the acquired data into physical values,
- the coherence between the parameters.

4.1. Time stamp

To detect a possible time shift in the data, the symmetry (with respect to solar noon) of the irradiance for very clear days is visually checked. When representing the solar irradiance versus the solar elevation angle h, the afternoon curve should normally lay over the morning curve. Exceptions do occur, however, at sites where the atmospheric turbidity changes during the day, due for example to topography-induced effects.

If this test is positive, verification can be done with the help of the global and beam clearness indices K_t and K_b. These parameters are plotted for the morning and afternoon data in different colours on the same graph. The upper limit, representative of clear-sky conditions, should lay over for the morning and the afternoon data as represented on Fig. 1 for one year of global irradiance data acquired at Carpentras. Ideal hourly clear-sky values, calculated with the Solis model, are plotted in blue on the same graph.

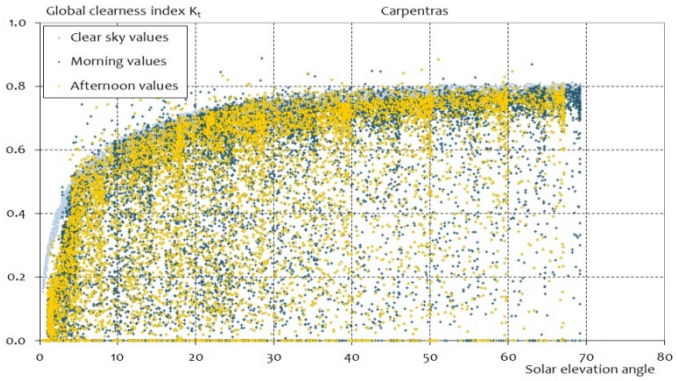

Fig. 1 K_t versus solar elevation angle

This test is very sensitive since a time shift of only a few minutes will conduct to a visible asymmetry.

When these two conditions are fulfilled, the time stamp of the data bank can be considered correct, and the solar geometry can be precisely calculated.

4.2. Sensors calibration

The sensors' calibration can be verified for clear sky conditions by comparison against data from a nearby station or with the help of additional measurements. To conduct this test, for each day, the highest hourly value of G_h and B_n is selected from the measurements and plotted against the day of the year as illustrated on Fig. 2. These points are representative of the clearest daily conditions. As the highest value for each day is selected, the upper limit normally represents clear-sky conditions. For G_h, it happens that higher-than-clear-sky values are obtained under partly cloudy or scattered clouds, high-sun conditions, this is why this test should not be applied for data with time granularity lower than one hour.

The sensor calibration's correctness can then be assessed by comparison if data from a nearby site are available. If not, this can alternatively be done with the help of a clear-sky radiative model when the atmospheric aerosol optical depth (*aod*) and the water vapor column (w) are known. The long term stability of the calibration can also be assessed with this method by plotting on the same graph several years of data.

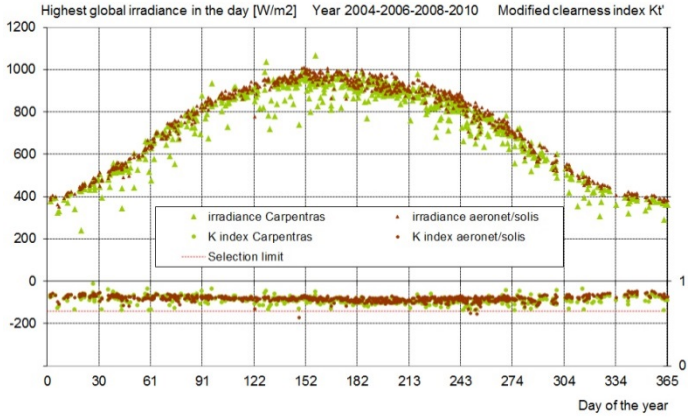

Fig. 2 Sensor's calibration assessment

4.3. Components consistency

The consistency test between the global and beam components can be verified with the help of their respective clearness indices. The hourly beam clearness index is plotted versus the corresponding global index as illustrated on Fig. 3. On the same graph, the clear-sky predictions from Solis clear sky model are represented for four different values of *aod*. The measurements (blue dots) should stay around the clear sky predictions.

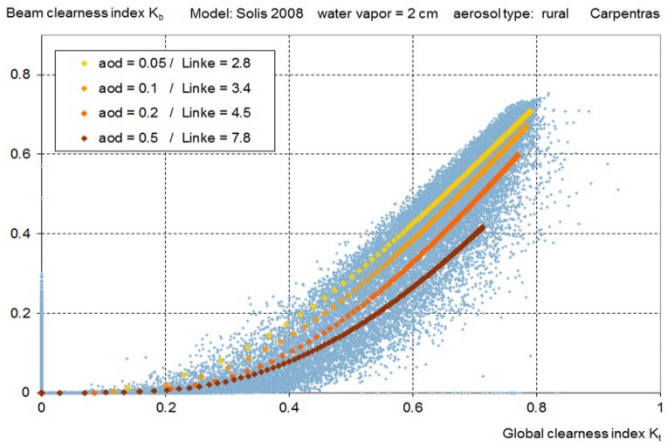

Fig. 3 K_b versus K_t: components consistency

5. Input parameters

The two main parameters needed to calculate clear sky irradiance are the atmospheric aerosol optical depth *aod* and the water vapour column *w*. The water vapour can be estimated from temperature ground measurements T_a and relative humidity *RH* with a ±15% uncertainty. This induces a less than ±2% uncertainty on the evaluated clear sky irradiance (Atwater 1976). The atmospheric aerosol content can be obtained either (i) from MACC-II project that monitors the global distributions and long-range transport of greenhouse gases such has carbon dioxide and methane, aerosols that result from natural processes and human activities, and reactive gases such as tropospheric O_3 and NO_2 (www.copernicus.eu), (ii) from spectral measurements with Cimel instruments through the Aerosol Robotic Network (aeronet), or (iii) by retrofit of the normal beam irradiance B_n with the help of Molineaux-Ineichen *bmpi* model described below. When the Linke turbidity factor is needed as input for a model, it is derived from *aod* and *w* using the conversion function developed by Ineichen (2002, 2008b).

From the station list, only three sites are part of the aeronet: Cabauw, Carpentras and Toravere, and two of them are situated at high latitudes. To circumvent the lack of ground aerosol optical depth measurements, measured irradiance data are used to estimate a daily aerosol optical depth by applying a retrofit on B_n. This can be done with the *bmpi* model. Based upon numerically integrated spectral simulations from Modtran (Berk, 1996), Molineaux (1998) derived two expressions for respectively the broadband optical depth of a clean and dry atmosphere and the water vapour optical depth. A classical exponential attenuation is then applied to evaluate the B_n.

To retrofit *aod* from B_n observations, the inverse model is applied in the following way: when the atmospheric water vapour column *w* is known, the hourly profile of B_n is calculated for each day and for the complete range of considered *aod*. Then, the daily profile with the lowest quadratic difference with the measurements is kept; it is related to the best fit of the daily *aod* value.

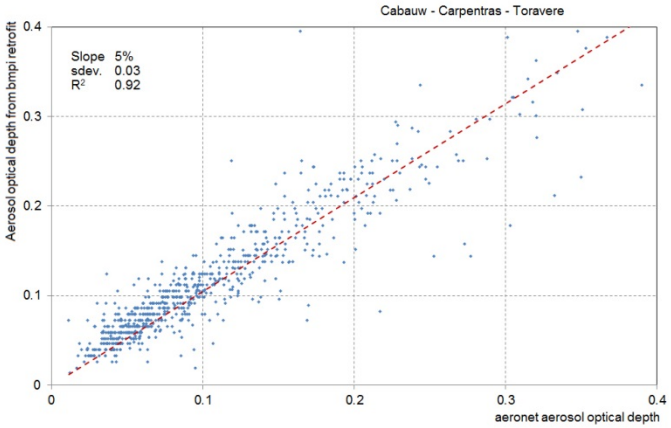

Fig. 4 Aerosol optical depths retrofit validation

The effectiveness of the method is illustrated on Fig. 4 where the retrofitted *aod* are plotted versus the aeronet measurements of the *aod*. The average slope is 5% away from the 1:1 diagonal, with a standard deviation of ±0.03 in optical depth units. The correlation coefficient is equal to 0.92.

6. Clear sky models validation results

In order to define physical limits for the measurements, the behaviour of the clear sky models and the coherence between irradiance components are analysed. To visualize these characteristics, model trends are represented for four typical values of aerosols optical depths (0.05, 0.1, 0.2 and 0.5) and a range of water vapour column; a value of w = 1cm is kept for the illustrations. An example is given on Fig. 5 for the Solis model, where the diffuse fraction D_h/G_h is represented versus the solar elevation angle.

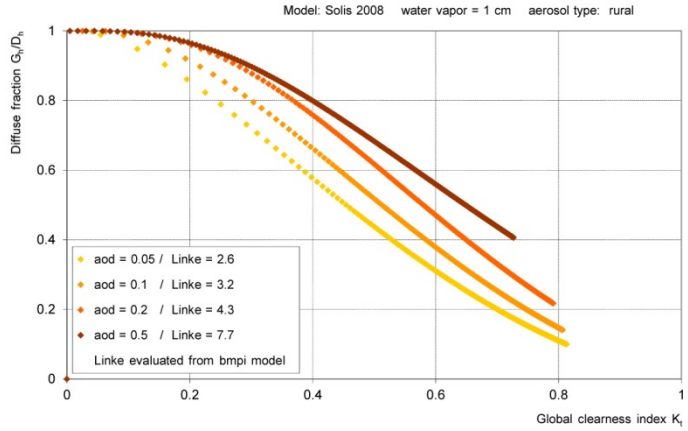

Fig. 5 Diffuse fraction for the Solis model

These Figures, done for each of the clear sky models, focus on small inconsistencies for some of the considered relationship:

discontinuous derivative due to LUT derivation, smooth inversion in the derivative of the global clearness index, incoherence of the global clearness index for low solar elevation angles, distorted diffuse fraction, etc. Solis is the only model that shows no inconsistency in any of the trends.

These effects occur mainly at low solar elevation angles and the consequences on the overall model precision are only minor. On the other hand, for some models, the consistency between the global and the beam components is not verified for low values of K_t (lower than 0.4 for the ESRA model).

The main validation results are the following:

• for the MACC-II aerosol source, the best results are obtained by the Solis model for the global component (-0.2%±2.4%) and by McClear for the beam component (-0.7% ±6.5%),
• for the *bmpi* aerosol source, respectively REST2 (0.5%±2.6%) and CPCR2 (-0.1% ±3.3%) give the best statistics.

The McClear model was developed with MACC-II aerosol data as input; it has to be noted that, when using MACC aerosol inputs, all the other models present a high negative bias and a high dispersion of the biases for the beam component. This expresses the fact that the MACC-II data presents some weaknesses in representing correctly the aerosol amount and/or the aerosol type. On the contrary, when using *bmpi* data as input, which are ground based measurements, the three REST2, CPCR2 and Solis give better results. Fig. 6 is an illustration of these results.

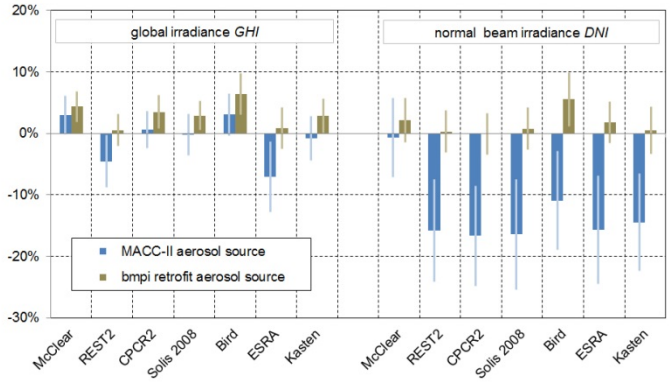

Fig. 6 Clear sky models validation results

7. All-weather models validation results

The validation is done on more than 500'000 hourly, 45'000 daily and 1'500 monthly values. The main results are that the hourly global irradiance is retrieved with a negligible bias and a standard deviation ranging from 17% to 24% (57 to 81[W/m2]), the beam component from 34% to 49% (119 to 174[W/m2]) with a -11% to +6% bias, and the diffuse from 35% to 60% (46 to 80 [W/m2]) with a bias from -10% to +25%. If the overall bias for the global irradiance models is near of zero, it can be highly variable from one site to the other. This is highlighted by the standard deviation of the mean bias deviation *sdb*; it varies from 2.1% to 5.1% for the global component. For the beam component (and a fortiori for the diffuse irradiance), the bias varies from site to site and model to model.

In a general way, for the global component and all the models, the bias distribution around the 1:1 axis follows a non- or slightly skewed normal distribution, so that the standard deviation indicator is significant. This is not the case for the normal beam irradiance bias, where bimodal, skewed or not normal distributions can occur depending on the model and the site. No common rule can be drawn; the shape of the distribution depends on the clear sky model used and the specificities of the input parameters. For some sites, the dispersion of the hourly B_n bias is so high that the distribution cannot be considered as normal. In this case, the standard deviation has to be considered with precaution. The observation of the bias versus the modified clearness index K_t' shows the same general tendency for all the models and both components: a slight overestimation for cloudy conditions and and a slight underestimation for very clear skies. The highest effect is a beam component overestimation for intermediate conditions. For clear conditions, the dispersion is due to an approximate knowledge of turbidity. In the case of intermediate cloud cover, the models do not identify with enough precision the type and thickness of the clouds. An illustration is given on Fig. 7.

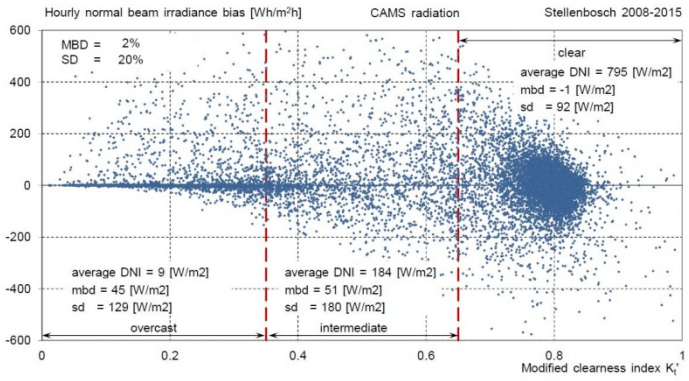

Fig. 7 Beam bias dependence with K_t'

None of the models shows a systematic dependence of the bias with the season or the aerosol load.

8. Interannual variability

The annual global and beam irradiation values are analysed year by year. A reference period covering the years 2004 to

2010 will guide the evaluation of the different products. The yearly total determined by the average over this reference period is used as normalization value for the annual totals of all the now casting and average models. The ground measurements annual standard deviation over this period is also calculated. Fig. 8 illustrates the method.

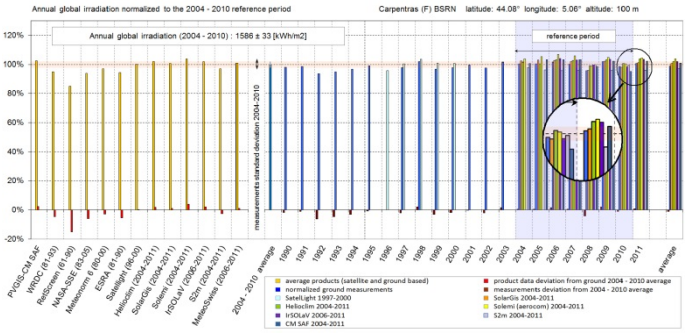

Fig. 8 Interannual variability

The following conclusions can be drawn from the validation for the global component:

- the overall bias for PVGIS-CM SAF and Meteonorm 7 is situated within ± one standard deviation of the interannual variability, with a bias standard deviation *sdb* around 4%,
- all the now casting models have a low bias, within ± one standard deviation of the interannual variability. The *sdb* varies from 2.1% to 5.1%,
- considering the site by site results, 60% of the site-model have a bias within ± one standard deviation of the interannual variability, 24% within ± two standard deviation, and 16% with a higher bias,

and for the beam component:

- the bias for NASA-SSE and Meteonorm 7 are within ± one standard deviation of the interannual variability with a *sdb* of respectively 9% and 12%,
- except Solemi, all the now casting models have an overall relatively low bias, within ± one standard deviation of the interannual variability. The corresponding *sdb* varies from 6% to 14%,
- considering the site by site results, 46% of the site-model have a bias within ± one standard deviation of the interannual variability, 29% within ± two standard deviation, and 25% with a higher bias.

9. Conclusion

A long term validation of hourly clear sky and all-weather models has been conducted with benchmarking data from 24 sites across Europe and Africa. Validation data cover up to 10 years. The main results of this investigation are the following:

- as expected, the main models uncertainties rely on the knowledge of the *aod* and *w*,
- Solis is the only **clear sky** model that shows coherence between B_n and G_h for all solar elevation angles,
- McClear, REST2 and Solis exhibit roughly the same performance: the standard deviation stays around ±3% for the global and ±4-5% for the beam component. The *sdb* are of the same order. All the models stay roughly within the measurement uncertainty for the global component,
- the **all-weather** hourly global irradiance is retrieved with a negligible bias and an average standard deviation around 17% for the best scheme. For B_n, the bias is around several percents, and the standard deviation around 34%,
- the *sdb* vary from 2% to 5% for the global irradiance, and from 6% to 14% for the beam component,
- for the majority of the sites, SolarGis, Heliomont and EnMetSol give the best statistics for all of the components,
- the bias dependence upon aerosol optical depth shows the same pattern for all models and locations,
- no general seasonal dependence could be observed.

Acknowledgements

This work is funded by the Swiss Energy Office.

References

Atwater M.A., Ball J.T. (1976) Comparison of radiation computations using observed and estimated precipitable water. J. Appl. Meteorol. 15, 1319-1320.

Berk A., Bernstein L.S. and Robertson D.C. (1996) «MODTRAN: a moderate resolution model for LOWTRAN 7», GL-TR-89-0122 (1989), updated and commercialized by Ontar Corporation, 9 Village Way, North Andover, Mass. 01845.

Bird R.E., Hulstrom R.L. (1980). Direct insolation models. Trans. ASME J. Sol. Energy Eng. 103, 182–192.

Cano, D., Monget, J., Albuisson, M., Guillard, H., Regas, N., & Wald, L.(1986). A method for the determination of the global solar radiation from meteorological satellite data. Solar Energy, 37, 31-39

Dagestad K. F. and Olseth J. A. (2007). A modified algorithm for calculating the cloud index. Solar Energy. 81, 280-289.

Dumortier D. (1995) Modelling global and diffuse horizontal irradiances under cloudless skies with different turbidities. Daylight II, JOU2-CT92-0144, Final Report Vol. 2.

Dumortier D. (1998) The Satellight model of turbidity variations in Europe. Technical Report Satellight Project.

ESRA (2000) European Solar Radiation Atlas, (2000) Fourth edition, includ. CD-ROM. Edited by J. Greif, K. Scharmer. Scientific advisors: R. Dogniaux, J. K. Page. Authors : L. Wald, M. Albuisson, G. Czeplak, B. Bourges, R. Aguiar, H. Lund, A. Joukoff, U. Terzenbach, H. G. Beyer, E. P.

Borisenko. Published for the Commission of the EC by Presses de l'Ecole, Ecole des Mines de Paris, France.

Fontoynont M. et al. (1998) Satellight: A WWW server which provides high quality daylight and solar radiation data for Western and Central Europe. Proc. 9th Conference on Satellite Meteorology and Oceanography, Paris, 25-29 May, 1998, 434–437.

Geiger M., Diabaté L., Ménard L.,Wald L. (2002) A web Service for Controlling the Quality of Measurements of Global Solar Irradiation. Solar Energy, 73 (6), 475-480.

Gueymard C. (1989) A two-band model for the calculation of clear Sky Solar Irradiance, Illuminance, and Photosynthetically Active Radiation at the Erath Surface. Solar Energy, Vol. 43, N° 5, 253-265

Gueymard C. (2001) Parametrized Transmittance Model for Direct Beam and Circumsolar Spectral Irradiance. Solar Energy Vol. 71, No. 5, 325–346

Gueymard C. (2004) High performance model for clear sky irradiance and illuminance. ASES Conference

Hammer A., (2000) Anwendungsspezifische Solarstrahlungsinformation aus METEOSAT-Daten, Dissertation, Universität Oldenburg, http://oops.uni-oldenburg.de/317/

Hammer A., Heinemann D., Hoyer C., Kuhlemann R., Lorenz E., Müller R., Beyer H.G. (2003): Solar energy assessment using remote sensing technologies. Remote Sensing of Environment, 86, 423–432.

Hammer A., Lorenz E., Kemper A., Heinemann D., Beyer H.G., Schumann K., Schwandt M. (2009): 'Direct normal irradiance for CSP based on satellite images of Meteosat Second Generation', SolarPACES 2009, Berlin

Ineichen P., Perez R. (2002) A new Airmass Independent Formulation for the Linke Turbidity Coefficient. Solar Energy, 73 (3), 151-157.

Ineichen P. (2008a) A broadband simplified version of the Solis clear sky model, Solar Energy, 82, 768-772.

Ineichen P. (2008b) Conversion function between the Linke turbidity and the atmospheric water vapor and aerosol content. Solar Energy 82, 1095–1097

Kalnay E. et al. (1996): The NMC/NCAR 40-year reanalysis project. Bull. Am. Meteorol. Soc. 77 (3), 437–472.

Kasten F. (1980) A Simple Parametrization of the Pyrheliometric Formula for Determining the Linke Turbidity Factor. Meteorol. Rdsch. 33, 124-127

Kasten F. (1984) Parametriesierung der Globalstrahlung durch Bedekungsgrad und Trübungsfaktor. Annalen der Meteorologie Neue Folge 20, 49-50

Kasten F. (1996) The Linke turbidity factor based on improved values of the integral Rayleigh optical thickness. Solar Energy 56 (3), 239–244.

Kinne S. et al (2005) An AeroCom initial assessment optical properties in aerosol component modules of global models Atmos. Chem. Phys. Discuss., 5, 1-46.

Lefèvre M. et al. (2013) McClear: a new model estimating downwelling solar radiation at ground level in clear-sky conditions. Atmos. Meas. Tech., 6, 2403–2418

Liu B.Y.H, Jordan R.C (1960) The interrelationship and characteristic distribution of direct, diffuse and total solar radiation. Volume 4, Issue 3, Pages 1-19

Lorenz E. (2007): Improved diffuse radiation model, MSG. Report for the EC-project PVSAT-2: Intelligent Performance Check of PV System Operation

Louche A., Notton G., Poggi P. and Simonnot G., (1991). Correlations for direct normal and global horizontal irradiation on a French Mediterranean site. Solar Energy. 46, 261-266.

Mayer B. and Kylling A. (2005) Technical note: The libRadtran software package for radiative transfer calculations – description and examples of use, Atmos. Chem. Phys., 5, 1855–1877, doi:10.5194/acp-5-1855-2005.

Meteonorm 6.1 (2009) Global Meteorological Database for Engineers, Planners and Education,

Molineaux B., Ineichen P., O'Neill N.T (1998). Equivalence of pyrheliometric and aerosol optical depth at a single wavelength. Appl. Opt., 37, 7008-7018.

Möser W. and Raschke E. (1984), Incident solar-radiation over europe estimated from meteosat data, J Clim Appl Meteorol, 23(1), 166–170.

Müller R., et al. (2004), Rethinking satellite-based solar irradiance modelling – the solis clear-sky module, Remote Sensing of Environment, 91(2), 160–174, doi:10.1016/j.rse.2004.02.009.

Oumbe A., Qu Z., Blanc P., Lefevre M., Wald L., 2014. Technical Note - Decoupling the effects of clear atmosphere and clouds to simplify calculations of the broadband solar irradiance at ground level. Geosci. Model Dev., in press.

Perez R., Ineichen P., Maxwell E., Seals R., Zelenka A. (1992) Dynamic global to direct irradiance conversion models. ASHARE Trans. Res. Series, 1992, 354-369

Remund J. (2009): Aerosol optical depth and Linke turbidity climatology, Description for final report of IEA SHC Task 36, Meteotest Bern

Rigollier C., Bauer O., Wald L. (2000) On the Clear Sky Model of the ESRA - european Solar Radiation Atlas - with Respect to the Heliosat Method. Solar Energy 68 (1), 33-48.

Rigollier C., Lefèvre M, Wald L. (2004) The method heliosat-2 for deriving shortwave solar irradiance radiation from satellite imagesSolar Energy, 77(2), 159-169

Stoekli R. (2013) The HelioMont Surface Solar Radiation Processing. Scientific Report, MeteoSwiss No. 93

Zarzalejo L.F., Polo J., Martín L., Ramírez L., Espinar B. (2009) A new statistical approach for deriving global solar radiation from satellite images. Solar Energy, Volume 83, Issue 4, Pages 480-484

Zelenka A., Perez R., Seals R. and Renné D. (1998) Effective accuracy of models converting satellite radiances to hourly surface insolation. Proc. 9th Conference on Satellite Meteorology and Oceanography, Paris, 25-29 May, 1998, 710–713.